Characterization of Silicone Elastomers for Refractive Field Grading under Sinusoidal Voltages

Jun Ting Loh, Stefan Kornhuber
University of Applied Sciences Zittau/Görlitz, Germany

Abstract

This contribution compares three different numerical approaches to characterize a nonlinear field dependent permittivity when stressed with a sinusoidal voltage. Silicone elastomers with refractive field grading properties serve as test samples. Their dielectric properties such as the DC-conductivity and the complex permittivity are determined experimentally and applied to compute the numerical models. Principally, all three models apply the *J-E* relationship to quantify the nonlinear permittivity, different numerical methods are however implemented to solve the models. The numerical approaches are compared with experimental results and analysed. Based on the results, the most suitable numerical method to determine the nonlinear permittivity could be determined. This model serves as a fundamental approach for sinusoidal voltages and can be further adapted for non-sinusoidal voltages in the future.

1. Introduction

Electric field grading is a common approach to reduce local field enhancement in the insulation system and thus essential to ensure the long-term reliability of an electric equipment. Different field grading methods are available, with their application depending on the voltage waveform. Field grading for standardized voltage waveforms such as DC-, sinusoidal- (AC) or transient voltages has been widely investigated [1]. A questionable case would be when non-standardized voltage waveforms arise, as current knowledge of field grading behaviour under non-standardized voltages are still limited. An example of non-standardized voltage is when harmonic frequencies ($AC_{x\,Hz}$) are present in the sinusoidal grid voltage ($AC_{50\,Hz}$), resulting in a distorted waveform.

Harmonics originate from power electronics, which find increasing usage in renewable energy equipment such as frequency converters. While the integration of power electronics allows higher flexibility and improved power transmission of electrical grids, harmonics pose as a new challenge to insulation systems of power equipment. For example, the study case from [2] shows that harmonics up to the frequencies of 12 kHz is the root of failure in cable terminations. The harmonic frequencies caused not only higher dielectric losses, but also increased temperature and "hot-spots" in the semiconductive field grading layer, leading to breakdown of the insulation system [2], [3]. While harmonics can induce a compromised field distribution in insulation systems with resistive field grading due to semiconductive materials, their influence of harmonics on refractive field grading materials remains unclear.

For refractive field grading, dielectrics are mixed with filler particles of higher relative permittivities such as carbon black or ferroelectrics ($\varepsilon_r > 10^4$), resulting in a composite material with a high permittivity ($\varepsilon_r > 15$) [4]. This allows refraction of the field equipotential lines in the case of field enhancement on the interface [1]. Naturally, this method is only effective in the case of a displacement field, such as with AC- or surge voltages. In addition, owing to the ferroelectrics, their permittivity is not only dependent on the frequency and temperature, they also exhibit a nonlinear field dependence [4]. The occurrence of harmonics where multiple frequencies and amplitudes are present could thus compromise the efficiency of the field grading.

An applicable model including the multiple frequencies and amplitudes of a harmonic distorted voltage would be beneficial for appropriate insulation design and in return guarantees the operational safety of the power equipment. For linear dielectrics, their behaviour can be fully described in the frequency domain [5] and as such can be simulated for example using the Finite-Element-Method [6], [7]. The model becomes more complicated in the case of field grading, where dielectrics then typically exhibit a nonlinear response such that the superposition theory becomes invalid. In terms of resistive field grading, the theory and practical applications of nonlinear conductance has been widely investigated [5], [8], [9]. For a nonlinear permittivity, a numerical model based on the analysis of the current density is introduced in [10] for sinusoidal voltages. However, there are still no numerical approach available to model a nonlinear field dependent permittivity under harmonic distorted voltages. This contribution compares multiple numerical approaches to model a nonlinear relative permittivity under sinusoidal voltages. The calculations are compared with experimental results to validate the methods. The proposed model serves as the basis and is to be adapted for harmonic distorted voltages in the future.

2. Theoretical background

Under an exciting sinusoidal voltage, the electric field $E(t)$ with the amplitude E is given as Eq. (1):

$$E(t) = E_0 \sin(\omega t) \qquad (1)$$

In terms of the electric field dependence, most dielectrics have a linear dielectric response (**Fig. 1(a)**). Based on the linear response theory, the effective current density can

be represented in the complex form with real and imaginary parts [11], [12]:

$$J = \sum_{i=0}^{\infty} J_i' \cos(i\omega t) + \sum_{i=0}^{\infty} J_n'' \sin(i\omega t) \quad (2)$$

With $J_i^{'}$ as the resistive J_{res} and $J_i^{''}$ as the displacement current density J_{cap}.

The complex quantities can be further translated into amplitudes, phase shifts as well as the dielectric properties such as the DC-conductivity σ_{DC} and permittivity ε_{r} [11]. The total current density J_{tot} and electric displacement D can then be described as below:

$$J_{\text{tot}} = J_{\text{res}} + J_{\text{cap}} = \sigma_{\text{DC}} E + \frac{\partial D}{\partial t} \quad (3)$$

$$D = \varepsilon_0 E + P_0 = \varepsilon_0 E + \varepsilon_0(\varepsilon_r - 1)E \quad (4)$$

with σ_{DC} as the DC-conductivity, ε_0 as the vacuum permittivity 8.854×10^{-12} Fm^{-1}, D as the electric displacement, and P_0 as the polarization at zero electric field. As the dipole moments of typical insulation materials such as epoxy or silicone elastomers cancel each other out at zero electric field [13], [14], P_0 is assumed to be zero.

When dielectrics behave nonlinear, for example due to effects such as ferroelectricity (nonlinear polarisation) or semiconductors (nonlinear conductance), the characterization of the dielectric with the linear response theory becomes insufficient. A nonlinear field dependence can be illustrated with the D-E loop, also known as the hysteresis curve (**Fig. 1(b)**)

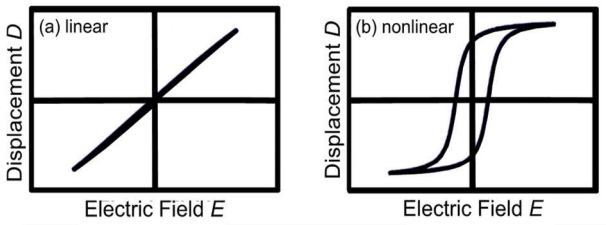

Fig. 1: Hysteresis loop for a linear dielectric **(a)** and a nonlinear dielectric such as a ferroelectric **(b)**

The *D-E* loop takes both the frequency and nonlinear field dependence into account and as such, can be used to quantify dielectric behaviour at high electric field strengths and at different frequencies [5], [15].

In the case of nonlinear permittivity, even under a sinusoidal voltage $U(t) = U_0\sin(\omega t)$, the displacement current becomes distorted (non-sinusoidal) due to the additional presence of higher harmonic terms $i > 1$ in Eq. (2). These harmonic terms can be represented as Fourier coefficients in the *D-E* relationship; the electric displacement D in Eq. (4) is then expressed using the Taylor series of the electric field E instead (Eq. (5) - (7)) [11], [14], [16]:

$$D = \varepsilon_0 \sum_{i=1}^{\infty} \varepsilon_{r,i} E_0^i \sin^i(\omega t) \quad (5)$$

$$D = \varepsilon_0(\varepsilon_{r,1}E + \varepsilon_{r,2}E^2 + \varepsilon_{r,3}E^3 + \cdots) \quad (6)$$

$$D(t) = \varepsilon_0\varepsilon_{r,1}E_0\sin(\omega t) + \varepsilon_0\varepsilon_{r,2}E_0^2\sin^2(\omega t) + \varepsilon_0\varepsilon_{r,3}E_0^3\sin^3(\omega t) + \cdots \quad (7)$$

Whereby Eq. (7) must be expanded and solved for all the present harmonic terms in the signal.

By applying Fourier transform and trigonometric expansion, the Taylor series of $D_i(t)$ for each harmonic term i can be determined:

$$D_1(t) = \varepsilon_0\left(\varepsilon_{r,1}E_0 + \frac{3}{4}\varepsilon_{r,3}{E_0}^3 + \frac{10}{16}\varepsilon_{r,5}{E_0}^5 + \cdots\right)\sin(\omega t) \quad (8)$$

$$D_2(t) = -\varepsilon_0\left(\frac{1}{2}\varepsilon_{r,2}{E_0}^2 + \frac{1}{2}\varepsilon_{r,4}{E_0}^4 + \cdots\right)\cos(2\omega t) \quad (9)$$

$$D_3(t) = -\varepsilon_0\left(\frac{1}{4}\varepsilon_{r,3}{E_0}^3 + \frac{5}{16}\varepsilon_{r,5}{E_0}^5 + \cdots\right)\sin(3\omega t) \quad (10)$$

With $\varepsilon_{\text{r,1}}$ as the linear relative permittivity, while the coefficients $\varepsilon_{\text{r,i}}$ at $i > 1$ define the nonlinear relative permittivity.

To determine $\varepsilon_{\text{r,i}}$ for each harmonic term i, the relationship between the electric current $I_{\text{cap}}(t)$ and electric displacement $D(t)$ is applied:

$$I_{\text{cap}}(t) = A_{\text{M}} \sum_{i=1}^{\infty} J_{\text{cap},i} = A_{\text{M}} \sum_{i=1}^{\infty} \frac{\partial D_i(t)}{\partial t} \quad (11)$$

$$I_{\text{cap},1}(t) = \underbrace{\varepsilon_0\omega A_{\text{M}}\left(\varepsilon_1 E_0 + \frac{3}{4}\varepsilon_3{E_0}^3 + \frac{10}{16}\varepsilon_5{E_0}^5 + \cdots\right)}_{I_1}\cos(\omega t) \quad (12)$$

$$I_{\text{cap},2}(t) = \underbrace{\varepsilon_0\omega A_{\text{M}}\left(\frac{1}{2}\varepsilon_2{E_0}^2 + \frac{1}{2}\varepsilon_4{E_0}^4 + \cdots\right)}_{I_2}\sin(2\omega t) \quad (13)$$

$$I_{\text{cap},3}(t) = \underbrace{-\varepsilon_0\omega A_{\text{M}}\left(\frac{1}{4}\varepsilon_3{E_0}^3 + \frac{5}{16}\varepsilon_5{E_0}^5 + \cdots\right)}_{I_3}\cos(3\omega t) \quad (14)$$

Where A_{M} is the effective area of the test sample.

With $E_0 = U/d$, where d is the sample thickness and U the amplitude of the voltage, the respective relative permittivity $\varepsilon_{\text{r},i}$ can be calculated:

$$\varepsilon_{r,1} = \frac{1}{\varepsilon_0\omega A_{\text{M}}}\left(\frac{d}{U}\right)^1\left(I_{\text{cap},1} + I_{\text{cap},3} + \cdots\right) \quad (15)$$

$$\varepsilon_{r,2} = \frac{1}{\varepsilon_0 \omega A_\mathrm{M}} \left(\frac{d}{U}\right)^2 \left(I_{\mathrm{cap},2} + I_{\mathrm{cap},4} + \cdots\right) \quad (16)$$

$$\varepsilon_{r,3} = \frac{1}{\varepsilon_0 \omega A_\mathrm{M}} \left(\frac{d}{U}\right)^3 \left(-\frac{4}{3} I_{\mathrm{cap},3} - 4 I_{\mathrm{cap},5} + \cdots\right) \quad (17)$$

In the further sections, this method of calculating the nonlinear relative permittivity by applying the *D-E* relationship and Taylor expansion is named as **Method 1 (M1)**.

Alternatively, under sinusoidal voltages, the displacement current density can also be calculated in Eq. (18) in [10], which takes into account of the field- and time dependent permittivity $\varepsilon_\mathrm{r}(E(t))$ [10], [17]:

$$J_\mathrm{cap}(t) = \frac{dD(t)}{dt} = \frac{d}{dt}\{\varepsilon_r(E(t)) \cdot E(t)\}$$

$$= E(t) \cdot \dot{E}(t) \cdot \dot{\varepsilon}_\mathrm{r}(E(t)) + \varepsilon_\mathrm{r}\big(E(t)\big) \cdot \dot{E}(t) \quad (18)$$

With $\dot{E}$ being the time derivative of the electric field and $\dot{\varepsilon}_\mathrm{r}$ being the time derivative of the permittivity as a function of $E(t)$. In terms of current $I(t)$ which can be determined experimentally, $\dot{\varepsilon}_\mathrm{r}(E(t))$ is given as:

$$\dot{\varepsilon}_\mathrm{r}(E(t)) = \frac{\frac{I(t) - I_\mathrm{res}(t)}{A_\mathrm{M}} - \varepsilon_\mathrm{r}\big(E(t)\big) \cdot \dot{E}(t)}{E(t) \cdot \dot{E}(t)} \quad (19)$$

With the derivative of relative permittivity $\dot{\varepsilon}_\mathrm{r}$ being a function of multiple variables (E and t), Eq. (19) takes the form of a first order differential equation. Under the condition that $E(t)$ is the inverse function of $t(E)$, Eq. (19) can be simplified and solved for $\varepsilon_\mathrm{r}(E)$ using partial integration [17]. It should be noted that this simplification is only valid when ε_r is not dependent on the frequency. As comparison with other calculation methods, this approach is also applied in this paper and is termed as **Method 2 (M2)**.

Besides that, a possible method to describe a nonlinear field dependent permittivity is by assuming a linear change of the permittivity as a function of the electric field strength. This can be implemented using a linear approximation of the permittivity **- Method 3 (M3)**.

This contribution solely focuses on the nonlinear permittivity, as such, the resistive current density J_res is a linear function of the electric field and will not be further discussed here. Theoretical approaches to evaluate a nonlinear conductivity can be found e.g. in [11] and [18].

3. Experimental approach

3.1 Test samples

As test samples, silicone elastomers filled with ferroelectrics particles (f-SiR) are used. A total of three plate form samples with the thickness $d = (1 \pm 0.05)$ mm are tested.

The experiments are conducted with a guard ring electrode arrangement with an effective area of $A_\mathrm{M} = 20$ cm^2. The samples are heated in an oven at 90 °C for 96 h before the start of every experiment to remove moisture in the sample.

3.2 Test method

Both the dielectric properties such as the DC-conductivity σ_DC and the relative permittivity ε_r are required to compute the model.

The DC-conductivity σ_DC of the test samples is measured using an electrometer (Keithley Multimeter 6517B) at voltages up to 1000 V_DC [19].

$$\sigma_\mathrm{DC} = \frac{Id}{U_\mathrm{DC} A_\mathrm{M}} \quad (20)$$

For the complex relative permittivity as a function of frequency, a middle frequency voltage is generated using a signal generator, amplified and transformed via a ferrite-core transformer (**Fig. 2**). The voltage and current is measured with a gas insulated capacitive voltage divider and a coaxial shunt (1 kΩ ± 5%). Both signals are sampled using a 16-bit data acquisition system (DAQ) at a sample rate of 2 MS/s for a total of three seconds.

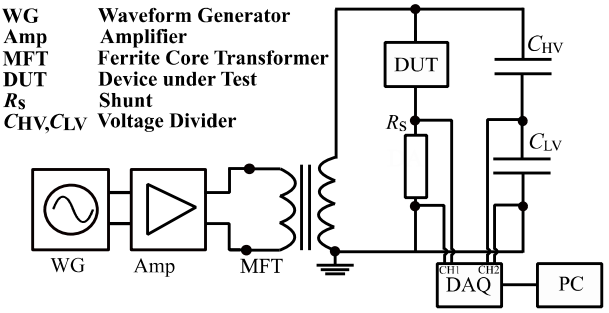

Fig. 2: Test setup for measurements of the voltage and current

By measuring the voltage $U(t)$ and current $I(t)$, the complex power can be calculated and separated into the active power P, apparent power S and reactive power Q. This way, the complex permittivity ε_r^*, consisting of the real ε_r' and imaginary permittivity ε_r'', is determined as:

$$P = \frac{1}{T} \int_0^t U(t) I(t) \quad (21)$$

$$S = U_\mathrm{rms} I_\mathrm{rms} \quad (22)$$

$$Q = \sqrt{S^2 - P^2} \quad (23)$$

$$\varepsilon_r' = \frac{Qd}{2\pi f A_\mathrm{M} {U_\mathrm{rms}}^2} \quad (24)$$

$$\varepsilon_\mathrm{r}'' = \varepsilon_\mathrm{r}' \tan\delta_\mathrm{DUT} = \varepsilon_\mathrm{r}' \frac{P}{Q} \quad (25)$$

At high frequencies, external error sources such as stray capacitance or inductance can cause inaccurate measurement results. To minimize such errors, a reference measurement as proposed in [6] is conducted before every test, whereby an air capacitor with very low loss ($\tan\delta < 10^{-4}$) is used as a test sample to record the

baseline loss angle δ_{ref} of the test setup. By removing δ_{Ref} from the measurement results, the corrected δ_{DUT} quantifies the true loss angle of the test sample.

4. Numerical model of an electric field dependent relative permittivity

Using **Method 1 (M1)**, the nonlinear complex relative permittivity can be computed based on the following steps. For the following example, an electric field strength $E_0 = 1$ kVmm^{-1} at the frequency $f = 350$ Hz is applied.

In spite of a sinusoidal excitation voltage $U_{meas}(t)$, the resulting current $I_{meas}(t)$ exhibits a distorted waveform. With the experimental results of the conductivity $\sigma_{DC} = 4.91\times10^{-11}$ at $E_0 = 1$ kVmm^{-1}, the total current is then separated into the resistive current $I_{res}(t) = \sigma_{DC}A_M E(t)$ and the displacement current $I_{cap}(t) = I_{res}(t) - I_{cap}(t)$ according to Eq. (3). It is seen that the distortion stems from the displacement current, indicating a nonlinear permittivity of the test sample (**Fig. 3**).

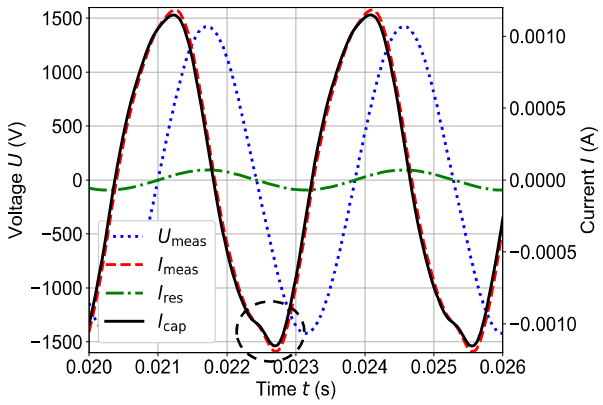

Fig. 3: Measured voltage U_{meas} and current I_{meas} signals at $f = 350$ Hz, with the separated resistive I_{res} and displacement current I_{cap}

It should be noted here that discrepancies in the measured results cannot be ruled out. The circle in **Fig. 5** highlights the distortion in form of a 'hump' in the negative half wave of the current signal, which is not observed in the positive half-wave. An assumption is high frequency noise in the voltage signal resulting in unwanted distortion of the sinusoidal waveform, consequently causing the hump in the current signal.

To determine the frequency spectrum of the current signal, a signal analysis is computed using Fast-Fourier Transformation (FFT), which shows the presence of harmonics up to the 5th term in $I_{cap}(t)$ (**Fig. 4**).

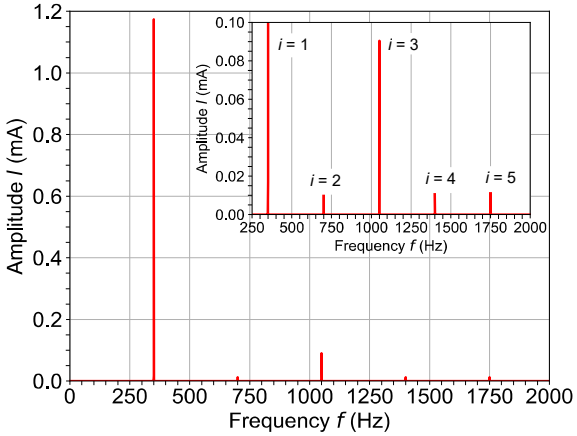

Fig. 4: FFT-Analysis of the current signal $I_{cap}(t)$ at $f = 350$ Hz, with the respective amplitudes at the harmonic terms $i = 1\ldots5$

An FFT-analysis also enables the determination of the magnitude and phase shift for each harmonic term ($i = 1\ldots5$). Consequently, the relevant real and imaginary parts of the complex current $I_i^* = I_i' + I_i''$ can be determined in order to calculate the complex relative permittivity $\varepsilon_{r,i}^*$ (**Table 1**) according to Eq. (15) - (17).

Table 1: Linear and nonlinear complex relative permittivity $\varepsilon_{r,i}^*$

$\varepsilon_{r,1}^*$ (Fm^{-1})	23.21 - j17.53
$\varepsilon_{r,2}^*$ (FV^{-1})	$4.77\times10^{-7} + j5.99\times10^{-7}$
$\varepsilon_{r,3}^*$ (FmV^{-2})	$-1.55\times10^{-12} + j5.24\times10^{-13}$
$\varepsilon_{r,4}^*$ (Fm^{2}V^{-3})	$-1.57\times10^{-19} + j8.33\times10^{-20}$
$\varepsilon_{r,5}^*$ (Fm^{3}V^{-4})	$1.82\times10^{-25} - j1.51\times10^{-25}$

It is important to note that for harmonic terms $i > 1$, $\varepsilon_{r,i}$ do not represent the material's relative permittivity at the frequency of the corresponding harmonic term i. Instead, they represent the coefficients relating D_i to E_i and as such, do not have any physical meaning.

5. Verification of the model

To verify the model, the measured current signal is compared with calculated signals using all three methods:

- **M1** – Based on the calculated complex relative permittivity $\varepsilon_{r,i}^*$ in **Table 1**, the current $I_{cap,i}(t)$ of every harmonic term can be calculated and summed up to form a total current $I_{M1}(t)$ (Eq. (11)).
- **M3** – The relative permittivity ε_r obtained from measurements (see Eq. (24)) is applied to calculate the displacement current.
  To avoid numerical error during computation, the time derivation of voltage $\dot{U}(t)$ is determined algebraically using Eq. (26):

$$\dot{U}(t) = 2\pi f \hat{U}_0 \cos(2\pi f t) \tag{26}$$

  With the field dependence of ε_r implemented by including a 15 % linear change of ε_r as a function of the electric field strength (Eq. (27)):

$$I_{M3}(t) = \varepsilon_r(1 + 0.15\sin(2\pi f t))\frac{\varepsilon_0 A_M}{d}\dot{U}(t) \quad (27)$$

The comparison of measured and calculated displacement current is shown in **Fig. 5**. Generally, **M1** and **M3** waveforms agree well with the measured signal, despite having different degrees of distortion. Interestingly, the hump in **Fig. 3** is not observed in all three computed signals, suggesting that it could stem from external factors. Other than that, it is noteworthy that the current signal reproduced using **M2** is pure sinusoidal, suggesting a linear behaviour of the material.

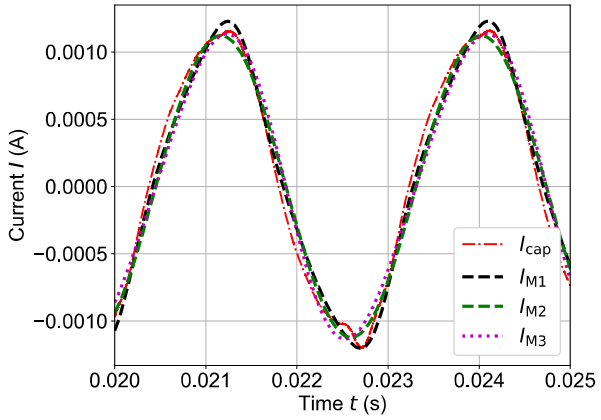

Fig. 5: Comparison of the measurement and the calculated displacement currents using three different methods

Additionally, the measured values such as the power loss P_δ and the real ε_r' and imaginary part ε_r'' of the complex relative permittivity are compared with calculated results using all three methods (Eq. (21) – (25)), with the relative error $\Delta x = (x_{Calc} - x_{Meas}) / x_{Meas}$ between the measured results and calculation also listed in **Table 2**.

Table 2:Comparison of the measured and calculated values of the power loss P_δ as well as the real ε_r' and imaginary part ε_r'' of the complex relative permittivity

Parameter	Meas.	M1	M2	M3
P_δ (W)	0.256	0.29	0.281	0.282
ΔP_δ (%)		13.3	9.8	10.2
ε_r' (Fm^{-1})	20.4	19.7	19.1	19.2
$\Delta \varepsilon_r'$ (%)		3.4	6.4	6.4
ε_r'' (Fm^{-1})	6.47	7.47	7.21	7.26
$\Delta \varepsilon_r''$ (%)		15.5	11.9	12

Among each other, all three calculation methods present comparable results with a maximum relative error of < 4 %. The discrepancies are higher when compared with the experimental results, with the highest being with **M1** at approximately 15.5 % for the values of ε_r'' (**Table 2**). The higher deviation between measurements and calculations could be attributed to the hump in the current signal as seen in **Fig. 3**. Nevertheless, **M1** has the lowest relative error of ε_r' at 3.4 %, proving its eligibility in determining nonlinear relative permittivities $\varepsilon_{r,i}^*$ with sufficient accuracy. Furthermore, the mathematical approach in **M1** which applies the Taylor series of the electric field strength E allows the additional quantification of the nonlinear relative permittivity $\varepsilon_{r,i}^*$ ($i > 1$), whereas with **M2** and **M3**, only the true complex permittivity ε_r^* can be determined.

In practice, such theoretical calculations of nonlinear relative permittivities $\varepsilon_{r,i}^*$ ($i > 1$) is useful for field grading design, mainly because these values can be further implemented in the Finite-Element-Method, thus allowing multiphysics simulations (i.e. thermal stress). Besides that, **M1** could also be easily adapted for an electrical stress under non-sinusoidal voltage waveforms. In the case of harmonic distorted voltages, the operational field strength would correspond to $E(t) = E_{50\,Hz}\sin(\omega t) + E_{x\,Hz}\sin(i\omega t)$ instead. With this in mind, **M1** is the preferred method to compute a numerical model for harmonic distorted voltages in the future.

6. Conclusion

The knowledge of a nonlinear field dependent permittivity is crucial information to ensure appropriate field grading design in insulation systems. In this contribution, three numerical methods are presented to determine a nonlinear field dependent permittivity, with their applications and limitations further discussed. A comparison with experimental results shows that the waveforms generally coincide well with each other. The numerical approach which applies the *D-E* relationship and the implementation of the Taylor expansion of field strength is proven to be a suitable method in the case of a sinusoidal voltage. Based on this model, an adapted numerical model to include harmonic distorted voltage is possible in the future.

Acknowledgements

The authors would like to thank BBC Cellpack Electrical Products for providing the specimens. This research was funded by the European Social Fund (ESF) and the Free State of Saxony.

References

[1] V. Hinrichsen and A. Küchler, "Grundlagen der Feldsteuerung," in *Feldsteuernde Isoliersysteme: Werkstoffe, Design, Prüfung und Simulation*, VDE Verlag GmbH, Darmstadt, 2011.

[2] L. Paulsson et al., "High-frequency impacts in a converter-based back-to-back tie; The Eagle Pass installation," *IEEE Trans. Power Deliv.*, vol. 18, no. 4, 2003.

[3] Li Ming, F. Sahlen, S. Halen, G. Brosig, and L. Palmqvist, "Impacts of high-frequency voltage on cable-terminations with resistive stress grading," in *Proceedings of the 2004 IEEE International Conference on Solid Dielectrics*, vol. 1, pp. 300-303, Jul. 2004.

[4] R. Bärsch and J. Kindersberger, “Nichtlineare dielektrische Funktionseigenschaften von Dielektrika,” in *Werkstoffe mit nichtlinearen dielektrischen Eigenschaften*, VDE Verlag GmbH, Stuttgart, Mar. 2008, vol. 110, pp. 7–33.

[5] T. Christen, L. Donzel, and F. Greuter, “Nonlinear resistive electric field grading part 1: Theory and simulation”, *IEEE Electr. Insul. Mag.*, vol. 26, no. 6, pp. 47–59, Nov. 2010.

[6] J. T. Loh and S. Kornhuber, “An Electro-Thermal Model for Dielectric Heating in Silicone Elastomers under Harmonic Distorted Voltages”, International Symposium on High Voltage Engineering ISH, Xi’an, China, Nov. 2021.

[7] M. Birle, “Beanspruchung von Polymeren durch höherfrequente Anteile einer Mischspannung,” Dissertation, Shaker Verlag, Aachen, 2015.

[8] A. Can-Ortiz, L. Laudebat, Z. Valdez-Nava, and S. Diaham, “Nonlinear Electrical Conduction in Polymer Composites for Field Grading in High-Voltage Applications: A Review,” *Polymers*, vol. 13, no. 9, Art. no. 9, Jan. 2021.

[9] L. Donzel, F. Greuter, and T. Christen, “Nonlinear resistive electric field grading Part 2: Materials and applications,” *IEEE Electr. Insul. Mag.*, vol. 27, no. 2, pp. 18–29, Mar. 2011.

[10] S. Blatt and V. Hinrichsen, “Mathematical model for numerical simulation of current density in microvaristor filled insulation materials,” *IEEE Trans. Dielectr. Electr. Insul.*, vol. 22, no. 2, pp. 1161–1170, Apr. 2015.

[11] T. Christen, R. Kochetov, and L. Almquist, “High-voltage low-frequency dielectric-spectroscopy used for characterization of nonlinear insulation materials,” in *2016 IEEE International Conference on Dielectrics (ICD)*, vol. 2, pp. 848–851, Jul. 2016.

[12] F. Kremer and A. Schönhals, *Broadband Dielectric Spectroscopy*, Springer Berlin Heidelberg, Berlin, 2003.

[13] E. Ivers-Tiffée and W. von Münch, *Werkstoffe der Elektrotechnik,* Teubner, Wiesbaden, 2007.

[14] Y. Li, J. Ho, J. Wang, Z.-M. Li, G.-J. Zhong, and L. Zhu, “Understanding Nonlinear Dielectric Properties in a Biaxially Oriented Poly(vinylidene fluoride) Film at Both Low and High Electric Fields,” *ACS Appl. Mater. Interfaces*, vol. 8, no. 1, pp. 455–465, Jan. 2016.

[15] V. Tomer and C. A. Randall, “High field dielectric properties of anisotropic polymer-ceramic composites,” *J. Appl. Phys.*, vol. 104, no. 7, p. 074106, Oct. 2008.

[16] T. Furukawa, K. Nakajima, T. Koizumi, and M. Date, “Measurements of Nonlinear Dielectricity in Ferroelectric Polymers,” *Jpn. J. Appl. Phys.*, vol. 26, p. 1039, Jul. 1987.

[17] S. Blatt, “Untersuchungen zu einem möglichen Einsatz von Mikrovaristoren in der Isolation umrichtergespeister Antriebe,” Dissertation, TU Darmstadt, Darmstadt, 2015.

[18] E. Martensson, “Modelling electrical properties of composite materials,” Dissertation, Kungl Tekniska Högskolan, Sweden, 2003.

[19] “DIN EN IEC 62631-3-1:2016 - Dielectric and resistive properties of solid insulating materials - Part 3-1: Determination of resistive properties (DC methods) Volume resistance and volume resistivity – General method”, Technical Report, Beuth Verlag: Berlin, Germany, 2016.